Synthesis and Property Behavior of Dioctyl Phthalate Plasticized Styrene–Acrylate Particles by Shirasu Porous Glass Emulsification and Subsequent Suspension Copolymerization

Roongkan Nuisin,[1] Shinzo Omi,[2] Suda Kiatkamjornwong[3]

[1]*Department of Materials Science, Faculty of Science, Chulalongkorn University, Bangkok 10330, Thailand*
[2]*Graduate School of Bio-Applications and Systems Engineering, Tokyo University of Agriculture and Technology, Tokyo 184-8588, Japan*
[3]*Department of Imaging and Printing Technology, Faculty of Science, Chulalongkorn University, Bangkok 10330, Thailand*

Received 20 November 2002; accepted 17 March 2003

ABSTRACT: Two-phase model styrene–acrylate copolymers were synthesized with a soft phase consisting of methyl acrylate, butyl acrylate, and butyl methacrylate. Besides the styrenic copolymers, copolymers containing a hard phase of methyl methacylate and methyl acrylate were also synthesized. Comonomer droplets with a narrow size distribution and fair uniformity were prepared using an SPG (Shirasu porous glass) membrane having pore size of 0.90 μm. After the single-step SPG emulsion, the emulsion droplets were composed mainly of monomers, hydrophobic additives, and an oil-soluble initiator, suspended in the aqueous phase containing a stabilizer and inhibitor. These were then transferred to a reactor, and subsequent suspension polymerization was carried out. Uniform copolymer particles with a mean diameter ranging from 3 to 7 μm, depending on the recipe, with a narrow particle size distribution and a coefficient of variation of about 10% were achieved. Based on the glass-transition temperatures, as measured by differential scanning calorimetry, the resulting copolymer particles containing a soft phase of acrylate were better compatibilized with a hard phase of methyl methacrylate than with styrene with dioctyl phthalate (DOP) addition. Glass-transition temperatures of poly(MMA-*co*-MA) particles were strongly affected by the composition drift in the copolymer caused by their substantial difference in reactivity ratios. Incorporation of DOP in the copolymer particles does not significantly affect the glass-transition temperature of MMA- or MA-containing copolymer particles, but it does affect the St-containing copolymer and particle morphology of the copolymers. J Appl Polym Sci 90: 3037–3050, 2003

Key words: suspension copolymerization; glass-transition; polystyrene; plasticizers; Shirasu porous glass (SPG)

INTRODUCTION

Polymer latices are the essential materials of the surface coatings industry. A large proportion of the commercially produced latex polymer has typically been used by being cast into films or acting as binders. Recent concerns for the environmental and safety effects have emerged from highly volatile organic compounds used in the traditional coating industry. The growing demand for waterborne coatings thus requires a substitution for solvent-based coatings. Properties of polymer films are affected by polymer type and its nature and film-preparation conditions. A coalescing agent is required to enable the latex particles to attract each other to form a continuous film. A core–shell polymer can be used to reduce the need for a coalescing solvent.[1,2]

Control of the latex particle morphology is important for many applications. Particle morphology is controlled by many factors, including the polymerization method, hydrophilicity of monomers and polymers, the particle viscosity,[3] the degree of grafting between the polymers,[4,5] and initiator properties and the mode of monomer addition.[6–9] Such heterogeneity could provide uniquely tailored properties, for example, dispersion of a soft, lower glass-transition temperature (T_g) latex, or a soft particle core entrapped in a matrix of a harder polymer shell, which can prevent cracks in the film as an impact modifier.[10–14]

Landfester et al.[1] investigated the polybutylacrylate (PBA)/poly(methyl methacrylate) (PMMA) system and found that the interface depends on different synthesis conditions and the size of the particles. The

Correspondence to: S. Kiatkamjornwong (ksuda@chula.ac.th).

Contract grant sponsor: Thailand Research Fund; contract grant number: 2.M.CU/42/E.1.

Contract grant sponsor: BASE, Tokyo University of Agriculture and Technology.

Journal of Applied Polymer Science, Vol. 90, 3037–3050 (2003)

core–shell latices are composed of the PBA soft core at room temperature and the rigid shell of PMMA. The T_g of PBA of −45°C is of course well below room temperature. PBA/PMMA (66 : 34) copolymer, or pure PBA (soft phase) as a seed in a two-stage emulsion polymerization with MMA (hard phase), was prepared by Kirsch et al.[2] The soft-to-hard phase ratio was varied over a wide range, and the influence of crosslinking the second-stage material was investigated.[14] The influence of the content and molecular weight of low-density polyethylene (LDPE) on dioctyl phthalate (DOP) plasticization in poly(vinyl chloride) (PVC) was studied. The plasticizing effects of DOP on the PVC plastisol were found to decrease with increasing LDPE content and LDPE molecular weight.[15] Uniform poly(styrene-*co*-MMA) [poly(St-*co*-MMA)] microspheres were prepared using the SPG (Shirasu porous glass) emulsification technique. The additives containing ester groups in the emulsion droplets demonstrated that the compatibility between the hydrophobic additive and the monomer was responsible for the varied morphologies of the particles.[15]

In the present study, the SPG emulsification technique and subsequent suspension polymerization were used in synthesis of poly(St-*co*-MA) and poly(MMA-*co*-MA), and poly(St-*co*-BMA) in the presence of DOP. The effect of the added DOP plasticizer on the copolymer morphology, glass-transition temperature, molecular weight, and particle size were studied.

EXPERIMENTAL

Materials

Styrene (Wako Pure Chemicals, Osaka, Japan) was reagent grade and stored at −10°C before use. Styrene monomer was distilled before use for Runs 2022–2052. Methyl methacrylate, methyl acrylate, butyl acrylate, and butyl methacrylate (Wako Pure Chemicals) were reagent grade and distilled to remove inhibitors before use. Polystyrene having a number-average molecular weight ($\overline{M}_n$) of 4200, a weight-average molecular weight ($\overline{M}_w$) of 40,000, and $\overline{M}_w/\overline{M}_n$ [or polydispersity index (PDI)] of 9.54 was produced in-house. Dioctyl phthalate (DOP, GC grade, Wako Pure Chemicals) was used as a plasticizer. *N,N′*-Azobisisovaleronitrile (ADVN, V65; Wako Pure Chemicals) and benzoyl peroxide (BPO; Kishida, Osaka, Japan) were used as initiators. Sodium dodecyl sulfate (SLS, biochemical grade; Merck, Darmstadt, Germany) and poly(vinyl alcohol) (PVA) having a degree of polymerization of 1700 and 88.5% saponification (Kuraray, Osaka, Japan) were used as the surfactant and stabilizer, respectively. Sodium nitrite ($NaNO_2$, reagent grade; Chameleon Chemicals, Osaka, Japan) and *p*-phenylenediamine (reagent grade; Chameleon Chemicals) were used as inhibitors. Sodium sulfate (Na_2SO_4, commercial grade; Kokusan Chemical Works, Tokyo, Japan) was used as electrolyte. Methyl alcohol (commercial grade; Wako Pure Chemicals) was used as a solvent and nonsolvent for the copolymers.

TABLE I
Standard Recipe for the SPG Emulsification

Component	Weight (g)
Continuous phase	
PVA-217	2.00,[a] 3.00[b]
SLS	0.10
Na_2SO_4	0.10
Inhibitor ($NaNO_2$, PDA)	0.04
Water	230
Dispersion phase	
Initiator (BPO, ADVN)	0.04
Total monomer content (St, MMA, MA, BA, BMA)	16.0
DOP	0.8

[a] SPG membrane pore size 0.51 μm.
[b] SPG membrane pore size 0.90 μm.

Emulsification procedure

An SPG membrane with a pore size of 0.51 or 0.90 μm (Ise Chemicals, Japan) was used for the emulsification. The preparative conditions for a one-step emulsification and experimental results are shown in Table I. Air pressure was used to permeate the dispersion phase from the SPG membrane. The pressure in a range of 1.28–1.45 kgf cm^{-2} for the 0.51- μm membrane and 0.30–0.70 kgf cm^{-2} for the 0.90-μm membrane were used. The dispersion phase containing a mixture of the monomers, DOP, and BPO (or ADVN) initiator was prepared. In a continuous phase, the PVA stabilizer, SDS surfactant, Na_2SO_4 electrolyte, and $NaNO_2$ inhibitor were dissolved. To prevent creaming of the droplets, the continuous phase was gently stirred at 300 rpm with a magnetic bar.

Polymerization

The emulsion obtained was transferred to a three-neck glass vessel with a capacity of 300 cm^3 connected with a semicircular anchor-type blade made of PTFE for agitation, a Dimroth condenser, and a nitrogen inlet nozzle. Nitrogen gas was gently bubbled into the emulsion for 1 h; the nozzle was lifted above the emulsion level. The temperature was increased to reach 75°C, and the emulsion was polymerized for 24 h under nitrogen atmosphere by suspension polymerization.

Characterization

Conversion of monomers

Percentage conversion of the monomer was monitored by a gravimetric method. Methyl alcohol was

TABLE II
Polymerization Recipe and Experimental Results for Styrene (SPG pore size 0.51 μm)[a]

Run no.	Composition	Monomer composition (wt %)	Monomer conversion (%)	D_e (μm)	CV_e (%)	D_p (μm)	CV_p (%)	$\overline{M}_n$ ($\times 10^{-4}$)	$\overline{M}_w$ ($\times 10^{-4}$)	PDI	T_g (°C) Clean	T_g (°C) Unclean
2013	PSt/DOP 2.5 wt % ADVN, $NaNO_2$	100	86.6	4.1	8.3	2.9	10.3	4.1	33.7	8.1[b]	18.1/71.0[c]	6.4/86.0[c]
2012	PSt/DOP 5 wt % ADVN, $NaNO_2$,	100	74.6	8.8	18.4	7.3	18.5	1.8	8.2	4.6	3.1/48.2[c]	1.0/43.1[c]
2014	PSt/DOP 5 wt % BPO, $NaNO_2$	100	76.5	6.3	15.2	5.9	11.2	1.7	3.9	2.3	12.7/77.4[c]	6.0/43.4[c]
2016	PSt/DOP 5 wt % ADVN, PDA	100	76.0	7.1	15.9	5.8	16.1	1.7	7.5	4.5	6.3/65.9[c]	11.7/54.8[c]

[a] D_e and D_p are diameters of emulsion droplets and polymer particles, respectively. CV_e and CV_p are coefficients of variation for emulsion droplets and polymer particles, respectively. $\overline{M}_n$ and $\overline{M}_w$ are the number-averaged molecular weight and weight-average molecular weight, respectively. PDI, polydispersity index.
[b] Bimodal peak.
[c] Two separate T_g values were observed.

added to precipitate the polymer. Polymer particles were separated by centrifugation at 2000 rpm and washed repeatedly with methyl alcohol two to three times. The polymer particles were dried under vacuum at room temperature for 48 h, after which they were weighed.

Surface morphology

The external morphology of polymer particles was observed by scanning electron microscopy (JEOL, Model JSM-5310, Japan). The specimens were prepared by diluting the polymer latex, from which the diluted suspension was dropped onto an aluminum stub surface and coated with a thin layer of gold under reduced pressure ($<10^{-2}$ Pa) using a fine coater (JEOL, Model JFC-1200). The magnification was set at $\times$2000 in the SEM micrographs taken for the determination of the average polymer particle size and coefficient of variation (CV).

Size and size distribution of emulsion droplets and polymer particles

Monomer droplets before polymerization were observed by optical microscopy (Olympus BHC optical microscope). Diameters of about 150 monomer droplets were measured to calculate an average diameter and a size distribution. The polymer particle sizes were measured by SEM techniques.

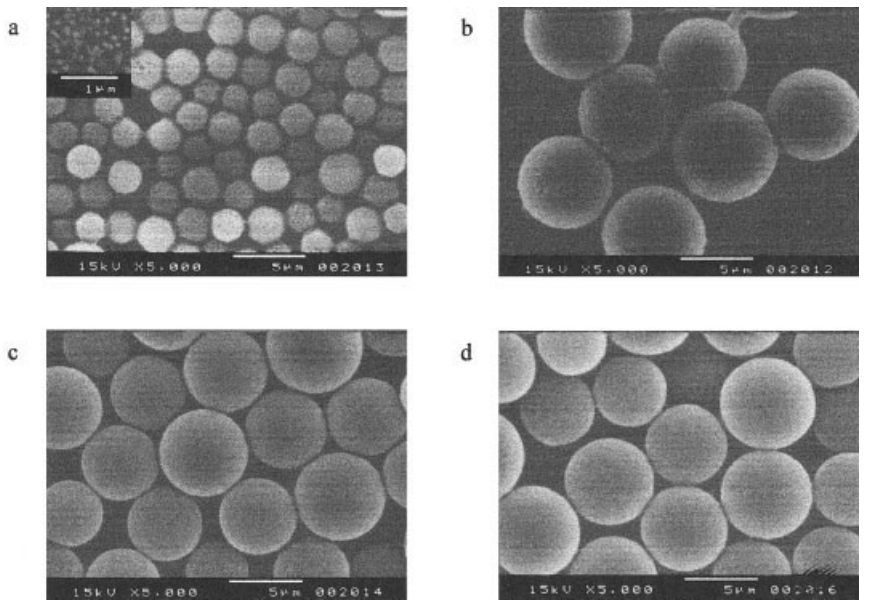

Figure 1 SEM micrographs of polystyrene incorporated with DOP: (a) DOP 2.5 wt % (Run 2013); (b) DOP 5 wt % (Run 2012, ADVN as initiator); (c) DOP 5 wt % (Run 2014, BPO as initiator); (d) DOP 5 wt % (Run 2016, ADVN as initiator and PDA as inhibitor).

TABLE III
Recipe and Experimental Results of Styrene and Methyl Acrylate Copolymerization

Run no.	Composition	Monomer composition (wt %)	Monomer conversion (%)	D_e (μm)	CV_e (%)	D_p (μm)	CV_p (%)	$\overline{M}_n$ ($\times 10^{-4}$)	$\overline{M}_w$ ($\times 10^{-4}$)	PDI	T_g (°C) Clean	T_g (°C) Unclean
2016[a]	PSt/DOP	100	76.0	7.1	25.9	5.8	16.1	1.7	7.5	4.5	6.3/65.9[b]	11.7/54.8[b]
2022	P(St-*co*-MA)	50/50	93.0	8.4	21.6	3.8	13.1[c]	2.0	4.4	2.2	23.2/65.4[b]	17.5/37.9[b]
2023	P(St-*co*-MA)	75/25	89.7	5.8	10.0	4.8	10.8	1.6	3.9	2.4	11.2/78.2[b]	11.0/47.5[b]
2046	P(St-*co*-MA)/DOP	52/48	17.4	6.5	15.3	5.8	16.5	0.4	1.6	4.5	21.1/55.1[b]	23.1
2028	P(St-*co*-MA)/DOP	75/25	52.2	7.1	16.1	5.9	19.7	1.6	3.6	2.3	24.9/58.3[b]	27.9
2024	P(St-*co*-MA)/PSt	37.5/50/12.5	89.8	7.8	21.1	5.2	15.8	1.3	3.8	2.8	26.7/72.2[b]	25.4/50.4[b]
2025	P(St-*co*-MA)/PSt	62.5/25/12.5	69.6	6.1	10.4	4.4	14.3	1.5	3.2	2.2	31.7/53.9[b]	20.9/49.9[b]
2029	[P(St-*co*-MA)/PSt]/DOP	37.5/50/12.5	38.9	7.0	16.1	5.0	18.3	1.2	3.2	2.8	22.2/50.1[b]	22.9/44.2[b]
2030	[P(St-*co*-MA)/PSt]/DOP	62.5/25/12.5	67.5	5.9	10.1	4.1	13.8	1.5	3.9	2.6	15.0/51.7[b]	14.6/46.9[b]

[a] SPG membrane pore size 0.51 μm; otherwise, 0.90 μm.
[b] Two separate T_g values were observed.
[c] Coagulated particles were partially observed.

On average, the diameters of 200 polymer particles were determined from SEM micrographs. Through the evaluation of the OM and SEM micrographs, the number-averaged diameters of the emulsion droplets (D_e) and polymer particles (D_p) were calculated according to eq. (1). In addition, the standard deviation (σ) and CV were calculated using the formulas expressed in eqs. (2) and (3). Here

$$D_n = \frac{\sum_{i=1}^{n} n_i D_i}{\sum_{i=1}^{n} n_i} \tag{1}$$

where n_i is the number of particles at diameters D_i, and D_n corresponds to the exact mean diameter of the population. The standard deviation σ is determined from the measured particle diameters in the following equation:

$$\sigma = \left[\frac{1}{n-1} \sum_{i=1}^{n} (D_i - D_n)^2 \right]^{1/2} \tag{2}$$

where i refers here to an individual particle.

The particle size distribution is reflected in the standard deviation. The breadth of the particle size distribution is proportional to the standard deviation of the particle diameters using the CV as follows:

$$\text{CV (\%)} = (\sigma / D_n) \times 100 \tag{3}$$

Internal morphology of the particles

The polymer particles of Runs 2018 and 2019 prepared from St : MA contents of 50 : 50 and 75 : 25, respectively, with incorporation of 5% DOP were subjected to TEM observation (JEOL, Model JEM 1010). The samples were microtomed and stained with RuO_4, and viewed at ×20,000 magnification.

Molecular weights and distribution

Gel permeation chromatography (GPC) was used for the examination of average molecular weights and the molecular weight distribution. The GPC chromatograms were obtained using Tosoh gel permeation chromatography (Model HLCH820 Chromato column; Tosoh, Tokyo, Japan) at the oven temperature of 40°C, and the injection temperature at 35°C. Pressure was applied to samples at 16 kgf cm^{-2} and reference was at 12 kgf cm^{-2}. There are two types of GPC columns for sample analysis. The first column (Model GRCX4) and the second column (Model GMMXL) were both packed with mixed gels of

TABLE IV
Recipe and Experimental Results for Methyl Methacrylate and Methyl Acrylate Copolymerization[a]

Run no.	Composition	Monomer composition (wt %)	Monomer conversion (%)	D_e (μm)	CV_e (%)	D_p (μm)	CV_p (%)	$\overline{M}_n$ ($\times 10^{-4}$)	$\overline{M}_w$ ($\times 10^{-4}$)	PDI	T_g (°C) Clean	T_g (°C) Unclean
2010	PMMA/DOP	100	85.6	6.9	25.9	Coag[b]	Coag[b]	3.7	13.0	3.5	14.0	14.0
2033	P(MMA-*co*-MA)	50/50	73.7	7.0	39.7	5.4	26.6	3.9	62.6	16.0[c]	25.9	29.4
2032	P(MMA-*co*-MA)	75/25	68.1	4.5	22.7	5.5	18.8	2.3	10.2	4.5	27.9	29.2
2035	P(MMA-*co*-MA)/ DOP	50/50	79.9	5.6	22.8	5.4	14.5[b]	4.0	52.3	13.2[c]	29.5	25.3
2034	P(MMA-*co*-MA)/ DOP	75/25	57.1	4.6	13.6	4.7	18.7	3.3	22.1	6.7	38.0	29.2

[a] SPG membrane pore size 0.9 μm.
[b] Coagulated particles were partially observed.
[c] Bimodal curve.

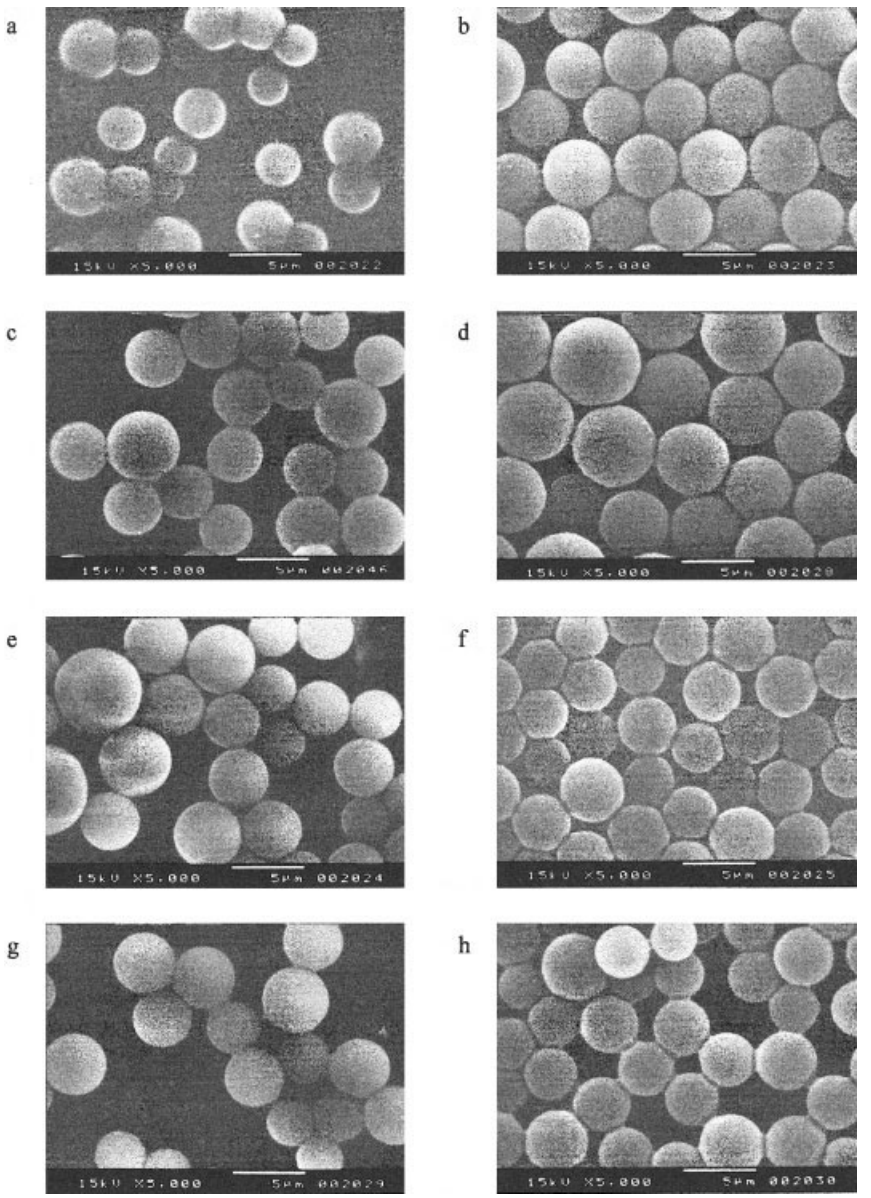

Figure 2 SEM micrographs of poly(St-*co*-MA): (a) St : MA = 50 : 50; (b) St : MA = 75 : 25; (c) St : MA = 52 : 48 with DOP; (d) St : MA = 75 : 25 with DOP; (e) St : MA : PSt = 37.5 : 50 : 12.5; (f) St : MA : PSt = 62.5 : 25 : 12.5; (g) St : MA : PSt = 37.5 : 50 : 12.5 with DOP; (h) St : MA : PSt = 62.5 : 25 : 12.5 with DOP.

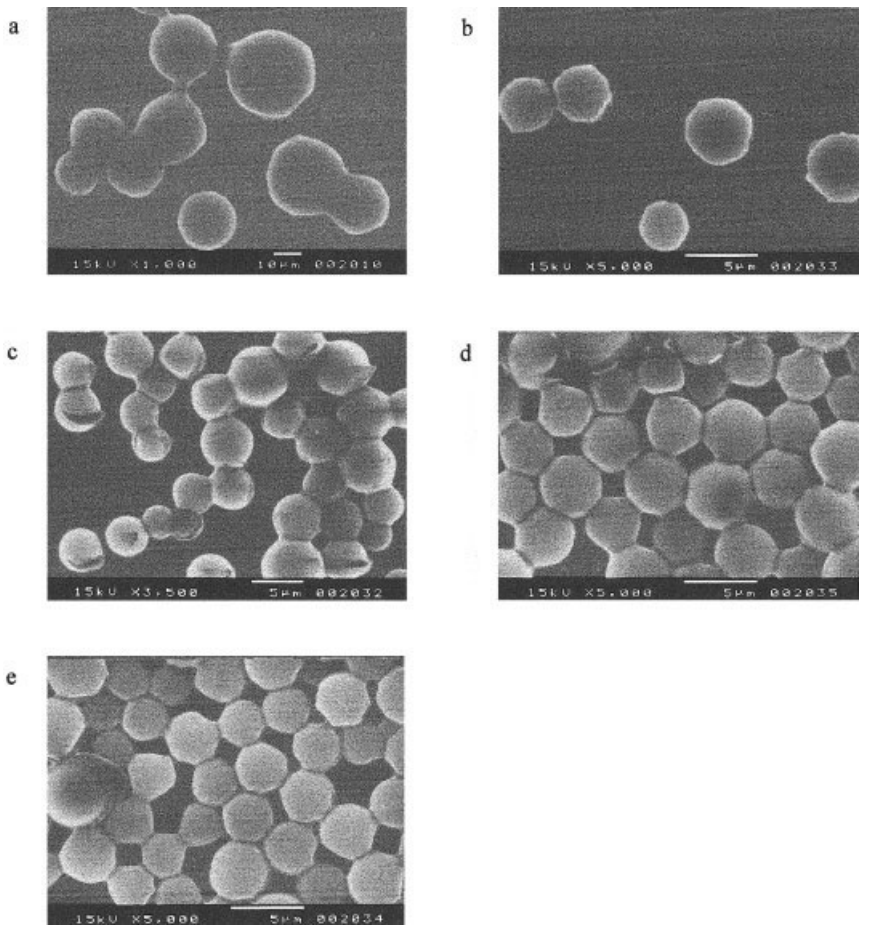

Figure 3 SEM micrographs of poly(MMA-*co*-MA): (a) PMMA–DOP; (b) poly(MMA-*co*-MA), MMA : MA = 50 : 50; (c) poly(MMA-*co*-MA), MMA : MA = 75 : 25; (d) poly(MMA-*co*-MA)–DOP, MMA : MA = 50 : 50; (e) poly(MMA-*co*-MA)–DOP, MMA : MA = 75 : 25.

poly(divinylbenzene-*co*-styrene). Likewise, the reference column (Model GMMXL) was also packed with mixed gels of poly(divinylbenzene-*co*-styrene). Tetrahydrofuran (THF, Wako Pure Chemicals) was used as solvent and eluent. For analysis, 1 mg of dried polymer sample was dissolved into 2 cm^3 of THF to obtain an approximate concentration of 0.1 wt %. Then the polymer solution, filtered with 0.2 μm PTFE membrane (Advantec, Tokyo, Japan), was injected into the columns at a flow rate of 0.5 cm^3 min^{-1}. The chromatogram was detected by a refractive index detector.

Glass-transition temperature

Measurements of glass-transition temperature (T_g) were performed using a differential scanning calorimeter (DSC, Model 3100; MAC Science). The sample was prepared by two methods, unclean and clean. For the first method, the polymer latex was dried under vacuum at ambient temperature for 120 h without further cleaning. For the second method, the polymer latex was washed repeatedly with methanol to remove all the surfactant and stabilizer. Then the precipitate latex was dried under vacuum at ambient temperature for 48 h. A sample (5–10 mg) from each preparation method was placed in the aluminum pan and put on the sensor at room temperature along with an empty pan as a reference to adjust the output balance. Measurement of the sample was performed at a heating rate of 10°C min^{-1}. The range of temperatures scanned was from −30 to 130°C.

RESULTS AND DISCUSSION

Effect of DOP on styrene homopolymerization

The polystyrene particles with DOP incorporated were prepared with an SPG membrane pore size of 0.51 μm for emulsification. They were subsequently polymerized by suspension polymerization. The preparative conditions for a one-step emulsification are shown in Table I and the recipes of copolymer compositions in Table II.

The SEM micrograph [Fig. 1(a) for Run 2013] shows that polystyrene particles incorporating DOP have an average diameter of 3 μm and are irregular in shape.

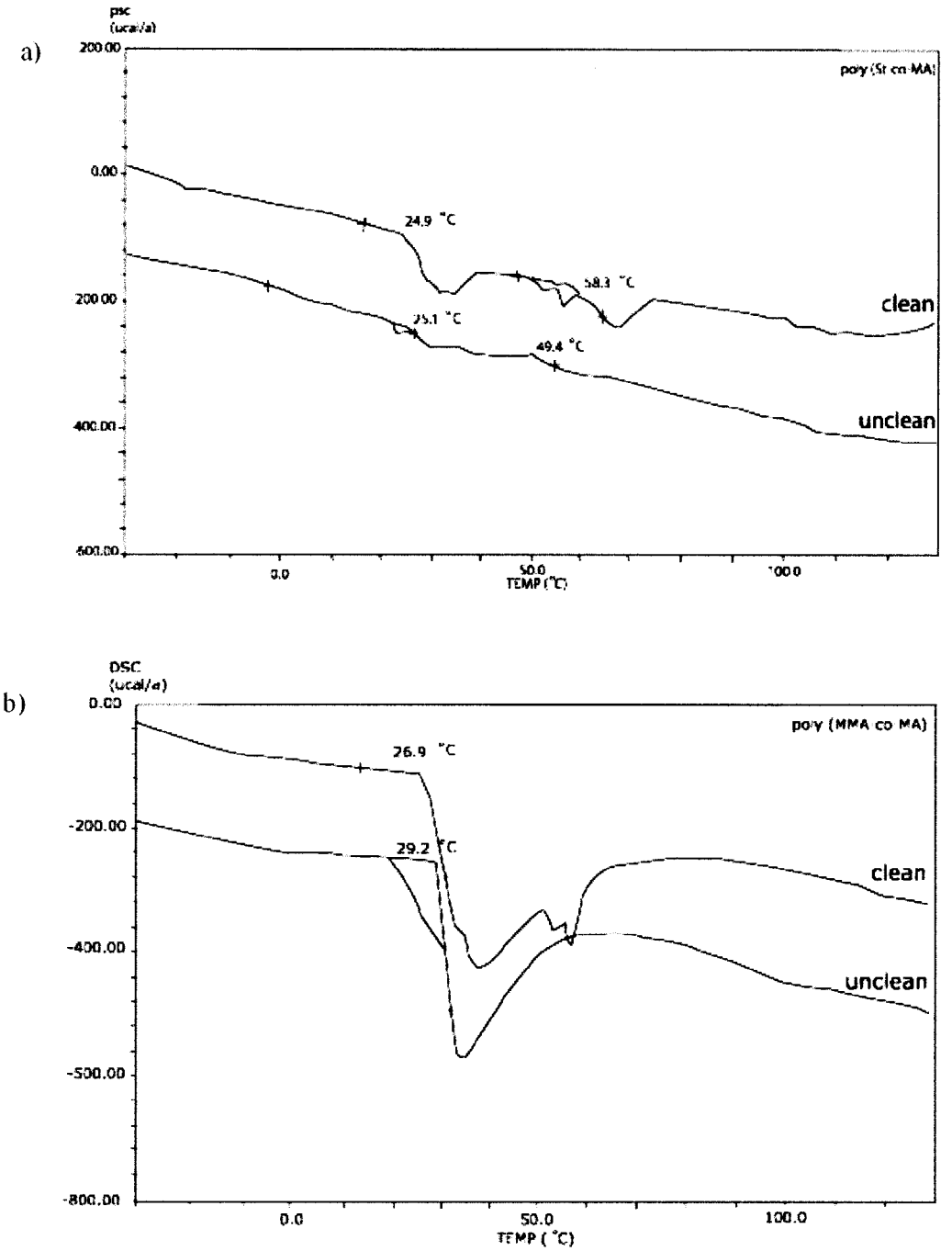

Figure 4 DSC thermograms of (a) poly(St-*co*-MA)–DOP and (b) poly(MMA-*co*-MA)–DOP.

A higher magnification of these particles revealed small particles with an average diameter of less than 0.1 μm. These small particles covered the surface of large particles. Very interestingly, we estimated that emulsion polymerization takes place at the expense of the suspension polymerization for the present case. Secondary particle nucleation in Run 2013 could take place at the longer emulsification time of 20 h using the SPG membrane pore size of 0.5 μm with low pressure (1.3 kgf cm^{-2}). Smaller emulsion droplets (4.1 μm) were obtained, leading to opalescence and formation of small polymer particles. This resulted in higher molecular weight and a bimodal molecular weight distribution. Because DOP and styrene monomers have relatively close solubility parameter values, both are thus compatible. As suspension polymerization proceeds, styrene polymerizes much faster and excludes DOP, leaving it in the aqueous phase because of the latter's moderate hydrogen bonding. The aqueous phase composition of dissolved styrene monomer and DOP then polymerized to give the minute amount of secondary particles deposited on the larger primary

TABLE V
Monomer Reactivity Ratios in Radical Copolymerization

M_1	r_1	M_2	r_2	r_1r_2
Styrene	0.84	Butyl acrylate	0.18	0.151
Styrene	0.19	Methyl acrylate	0.80	0.154
Styrene	0.56	Butyl methacrylate	0.31	0.174
Styrene	0.52	Butyl methacrylate	0.47	0.244
Styrene	0.74	Butyl methacrylate	0.59	0.437
Styrene	0.49	Methyl methacrylate	0.418	0.205
Methyl methacrylate	2.15	Methyl acrylate	0.40	0.86

particles. Glass-transition temperatures of the composite polymer as shown in Table II, corresponding to the highly and modestly plasticized portions, are 18 and 71°C, respectively. The glass-transition temperature results confirm the polymerization loci. We anticipate that DOP migration could probably take place during the temperature rise in the course of the DSC measurement.

Dependency of styrene homopolymerization on the initiator type

Two types of initiator, ADVN (a more aqueous type) and BPO (a nonaqueous type), were used to polymerize DOP plasticized styrene. Both initiators produced similar monomer conversions of 74.6 and 76.5%. The effects of the initiator on the particle size are shown in Table II. The average particle size obtained from ADVN initiation [Run 2012, Fig. 1(b)] was larger than that from BPO [Run 2014, Fig. 1(c)]. After the polymer latex had been kept for 24 h, we found that the plasticized polystyrene synthesized with BPO initiation gave one layer of precipitate residing at the bottom of the bottle. In contrast, two separate layers of precipitate were observed for the ADVN initiation. The BPO-initiated polystyrene preferred not to suspend in the aqueous phase because of the higher hydrophobicity of both initiator fragments. For the ADVN initiation system, the polystyrene particles with the more polar initiator fragments could better remain in the aqueous phase. Therefore, BPO initiation gave polymer with lower average molecular weights and a narrow molecular weight distribution than those from the ADVN initiation because the former terminated faster than did the latter. However, the surface morphology of the polymer particles was still similar because a smooth surface was obtained as shown in Figure 1(b)–(d).

The glass-transition temperature of DOP plasticized polystyrene is presented in Table II. For all experiments, two separate T_g values were found, indicating increasing immiscibility of the styrene monomer (dissolving PS) and DOP during polymerization. At the beginning stage of the polymerization, more DOP concentration was used along with styrene conversion because the polymer chain lengths were still short, which eased the inclusion of DOP between these chains. At this stage, highly plasticized polystyrene was obtained, yielding a lower glass-transition temperature. At the later stage of polymerization, less DOP was retained in the monomer droplets. Less-plasticized polystyrene particles (chains) resulted, yielding a higher glass-transition temperature.

Effect of the inhibitor on polymerization and polymer particles

Two types of water-soluble inhibitors, $NaNO_2$ and PDA, were used.[16] From Table II it may be observed that the inhibitors did not significantly affect the monomer conversion, molecular weights and distribution, and particle morphology. All the synthesized particles had smooth surfaces and were spherical with

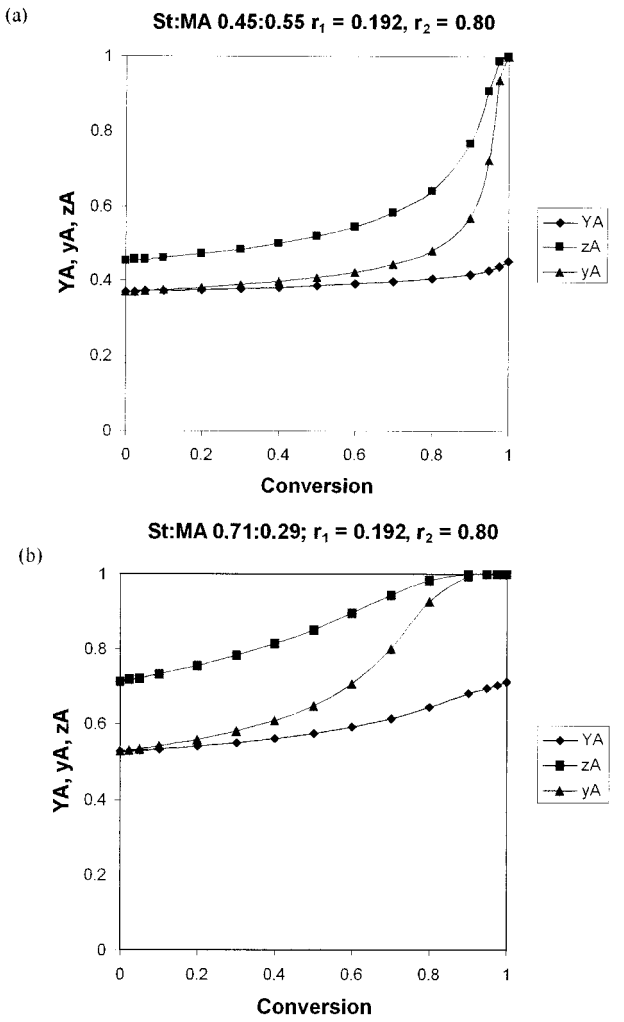

Figure 5 Composition drift of poly(St-*co*-MA): (a) St : MA, 50 : 50 wt %; (b) St : MA, 75 : 25 wt % (YA, cumulative composition of styrene in copolymer; yA, composition of styrene in unreacted monomer; zA, instantaneous composition of styrene in copolymer).

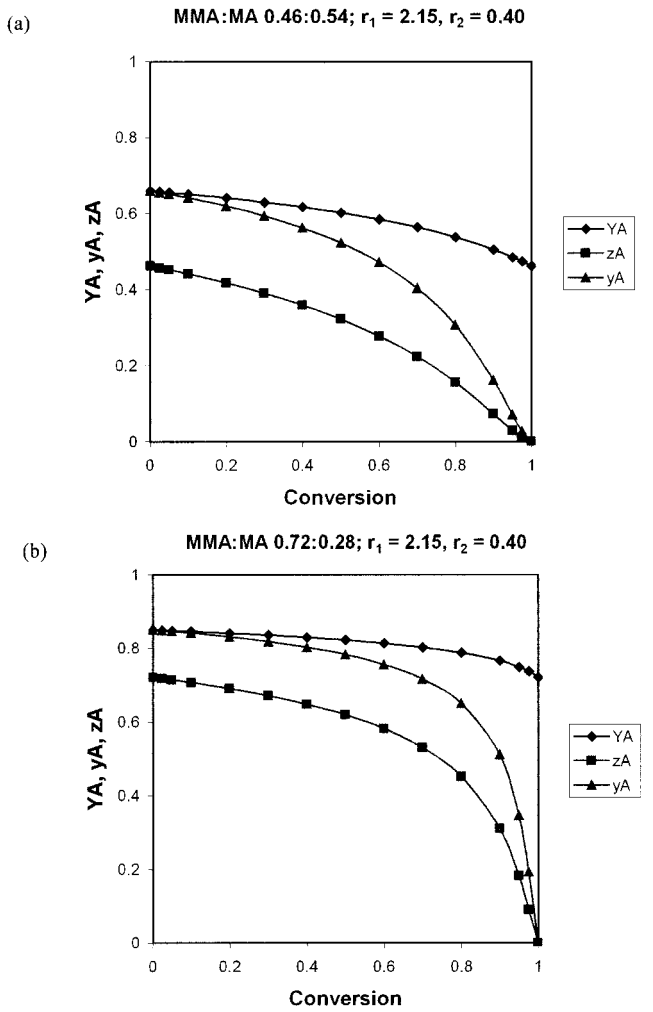

Figure 6 Composition drift of poly(MMA-*co*-MA): (a) MMA : MA, 50 : 50 wt %; (b) MMA : MA, 75 : 25 wt % (YA, cumulative composition of MMA in copolymer; yA, composition of MMA in unreacted monomer; zA, instantaneous composition of MMA in copolymer).

an average particle size of 8 μm. One must mention that the latex with a PDA inhibitor exhibited a dark violet color [Fig. 1(d)], from which dark brown polystyrene particles resulted. For the forthcoming syntheses of plasticized copolymers, only $NaNO_2$ was used as an inhibitor.

Effect of DOP on properties of poly(styrene-*co*-MA) and poly(MMA-*co*-MA) particles

Particle morphology

DOP plasticizer of 5% by weight of monomer was added to 16 g of total monomer mixtures. Poly(St-*co*-MA) and poly(MMA-*co*-MA) particles were then synthesized as shown in Tables III and IV. SEM micrographs for all copolymer particles obtained in each run are shown in Figure 2. The particles of poly(St-*co*-MA) remained spherical in shape as shown in Figure 2(a)–(d). In the absence of DOP, pinholes on the particle surface were observed in Figure 2(a) for Run 2022. In addition, small flakes were attached to the particle surfaces in Run 2023 [Fig. 2(b)] when the amount of styrene monomer increased in the absence of DOP. With the addition of DOP, the polymer particles retained a spherical shape with a smooth surface. Poly(MMA-*co*-MA) was synthesized by use of the same experimental methods as for the poly(St-*co*-MA). A smooth, spherical particle surface was obtained for all recipes. However, the particles were soft and easily deformed when exposed to a strong electron beam from the SEM apparatus as shown in Figure 3. Poly(St-*co*-MA) particles are rather strong and rigid because its vinyl backbone contains the bulky phenyl group moiety as a substituent group for the hydrogen atom, whereas poly(MMA-*co*-MA) particles are relatively flexible, with the less-stiff and weaker aliphatic functional group. This difference in chain stiffness could be the reason for the polymer surface hardness and resistance to high energy irradiation.

Glass-transition temperature

The secondary (higher) T_g value of the unclean poly(St-*co*-MA) particles was found (Table III and Fig. 4) to be lower than that of the clean polymer. The glass-transition temperature of polymers is of course affected by the addition of DOP plasticizer (5 wt % of monomer). In general, DOP resides physically inside the polymer chains and reduces the repulsion force between intermolecular chains. It can thus ease the motion of the rigid chains of styrene–MA copolymer. In comparison, some portions of DOP in the polymer latex cleaned with methanol were washed out from the particles during the treatment. The secondary T_g of the clean polymer particles was higher than that of the unclean latex, which was close to the T_g value of neat polystyrene homopolymer. Besides the removal by methanol cleaning, migration of the DOP plasticizer to the particle surface according to its general nature may assist in the removal during the cleaning. On the other hand, the primary (lower) T_g values were located close to the T_g of the MA homopolymer, depending on the MA monomer content in the copolymer. The different increments in T_{g1} (the lower T_g) and T_{g2} (the higher T_g) depended greatly on the sample preparation methods and the incorporated amount of DOP. The difference between T_{g1} and T_{g2} of the clean particles was greater than that of the unclean particles. In addition, the T_{g1} and T_{g2} of the DOP plasticized polymer particles were narrower than those of particles without DOP.

Table V shows the reactivity ratios of the comonomers in the present research. Figure 5 shows the composition drift of St in the copolymer of poly(St-*co*-MA).

TABLE VI
Recipe and Experimental Results of Styrene and Butyl Methacrylate Copolymerization

Run no.	Composition	Monomer composition (wt %)	Monomer conversion (%)	D_e (μm)	CV_e (%)	D_p (μm)	CV_p (%)	$\overline{M}_n$ ($\times 10^{-4}$)	$\overline{M}_w$ ($\times 10^{-4}$)	PDI	T_g (°C)	
											Clean	Unclean
2002[a]	P(St-*co*-BMA)	80/20	63.8	7.1	25.9	5.8	16.1	4.9	57.9	11.9[b]	na	26.1/45.7[c]
2008[a]	P(St-*co*-BMA)	50/50	71.8	8.4	21.6	3.8	13.1	1.5	5.2	4.0	12.2/43.8[c]	−3.0
2051[d]	P(St-*co*-BMA)/PSt	(62.5/25)/12.5	75.4	8.4	14.7	6.1	20.9	0.5	3.4	6.9	23.8/58.4[c]	17.2/65.7[c]
2052	P(St-*co*-BMA)/PSt	(62.5/25)/12.5	52.0	6.2	17.5	5.5	21.2	0.5	2.8	5.2	21.2/50.0[c]	17.3

[a] SPG pore size 0.51 μm; otherwise, 0.90 μm.
[b] Bimodal peak.
[c] Two separate T_g values were observed.
[d] Recipe without DOP. na, not available.

The reactivity ratios of the two monomers, r_1 (St = 0.192) and r_2 (MA = 0.80),[17,18] indicate that MA is consumed faster than St [Fig. 5(a)]. The reaction mixture is short of MA, that is, the polymer propagation chains are rich in MA units at the beginning [Fig. 5(b)], and the subsequently growing chains are terminated by the St monomer units when approaching a complete conversion. The composition drift of styrene was more pronounced at the higher styrene concentrations. Based on $r_1 r_2 \approx 0.15$, this copolymer lies between the two extremes of ideal and alternating copolymerization.[18] As the $r_1 r_2$ product decreases from unity (1 for an ideal copolymerization) toward zero, there is an increasing tendency toward alternation. However, the copolymer is still of a random type. Copolymer composition drift could be an attribute determining the extent of T_g in 50/50 wt % of poly(St-*co*-MA) as shown in Table III.

In the case of poly(MMA-*co*-MA), a single T_g value with a sharp transition was observed for all copolymer compositions as shown in Figure 4(b). The T_g value was close to room temperature. T_g values of the copolymers with and without DOP were observed in the same range, as shown in Table IV. Likewise, the T_g value is also controlled by the composition drift in the copolymer. Moreover, a much greater composition drift in the copolymer is also found in the case of MMA–MA monomers. The reactivity ratios of MMA (r_1) and MA (r_2) are 2.150 and 0.400,[17,18] respectively, as shown in Table V. Based on the $r_1 r_2$ product of 0.86 (approaching 1), poly(MMA-*co*-MA) is an ideal (random) type of copolymer. Figure 6 shows the composition drift of MMA in the copolymer. Because the MMA reactivity ratio is greater than unity, the copolymer contains a larger proportion of MMA [Fig. 6(a)]. The very high value of r_1 produces the MMA-rich chains at the beginning of the copolymerization [Fig. 6(b)], which causes MMA starvation in the reaction mixture. At the end of the copolymerization, MA units are thus preferentially consumed, depending on the reaction time. Because the difference in reactivity of the two monomers is very high, it becomes more difficult to produce copolymers having appreciable amounts of the less-reactive monomer, unless the copolymerization approaches the end of conversion. Composition drift in the copolymer is thus another factor that controls the glass-transition temperature of the copolymer.

Compared with poly(St-*co*-MA), poly(MMA-*co*-MA) copolymers achieved better compatibility than that of St–MA copolymers. This could result from the similar chemical structure of DOP and acrylate monomer. In other words, the DOP mixes more homogeneously in the matrix of poly(MMA-*co*-MA) than it does in the matrix of poly(St-*co*-MA), according to the DSC thermograph shown in Figure 4.

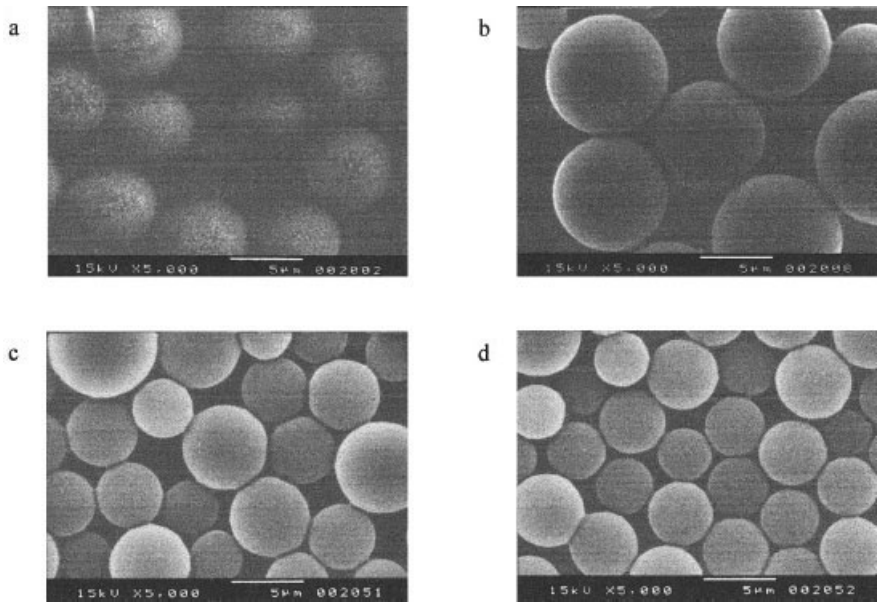

Figure 7 SEM micrographs of poly(St-*co*-BMA)–DOP: (a) St : BMA = 80 : 20; (b) St : BMA = 50 : 50; (c) St : BMA : PSt = 62.5 : 25 : 12.5 (without DOP); (d) St : BMA : PSt = 62.5 : 25 : 12.5.

However, other factors influencing T_g may include the surfactant and stabilizer in the polymer latex,[19] given that the PVA and SLS can physically adsorb onto the polymer surface. If possible, it might be necessary to separate the particles from their serum before proceeding to the subsequent processes. The heating rate during the DSC scanning is also undoubtedly one of the factors that governs the T_g value.

Effect of the addition of polystyrene on properties of poly(St-*co*-BMA) copolymers

The SPG membrane pore size of 0.90 μm was used for the emulsification of St and BMA, with results as shown in Table VI. The amount of the BMA phase was varied from 20 to 50% in the monomer mixture in the presence of 5 wt % DOP of total monomer mixture. When the BMA phase is present at more than 50 wt %, the particles become flattened, which is in agreement with our previous work.[15,20] SEM micrographs of the poly(St-*co*-BMA) particles are shown in Figure 7. Spherical particles having smooth surfaces were synthesized without a phase separation. Upon the addition of 12.5 wt % polystyrene (with $\overline{M}_n$ = 4000; $\overline{M}_w$ = 40,000) into the St–BMA mixture, the viscosity of the dispersion phase significantly increased. The number-averaged molecular weight of the resulting copolymer was close to 5000 as shown in Table VI (Runs 2051 and 2052). We anticipate that added polystyrene functions as if it were a macromonomer (a bulky molecule), which diffuses rather slowly in the monomer mixture. Because it is of rather high molecular weight, polystyrene thus retards the propagation step of St and BMA monomers. Therefore, the higher molecular weight polystyrene can be considered as a kind of molecular spacer to prevent the propagating radicals from adding more monomers. The most likely outcome for these short propagating radicals is to terminate, which ultimately results in a low average molecular weight.

When methanol was added into the reaction mixture, all the polymer components containing styrene units were precipitated to result in a mixture of poly(St-*co*-BMA) and polystyrene beads. This mixture of the plasticized poly(St-*co*-BMA) and polystyrene increased the glass-transition temperatures of the particles. As shown by the second T_g of the clean particles in Runs 2051 and 2052, the addition of polystyrene in the reaction mixture does not significantly alter the efficiency of DOP in poly(St-*co*-BMA)/PSt. Thus it is not necessary to include DOP in the composite particles of poly(St-*co*-BMA) when polystyrene is added before the polymerization.

Glass-transition temperature of poly(St-*co*-BMA)

A single-stage glass-transition temperature was revealed in the unclean poly(St-*co*-BMA) copolymer as shown in Table VI. The presence of DOP in the copolymer enhances the free volume of the hard phase. Because both DOP and BMA contain a similar ester functional group, the DOP can be compatible with the BMA soft domain. In each domain, the DOP molecular chains lubricate the St backbone, resulting in a low single T_g in both poly(St-*co*-BMA)/PSt and poly(St-*co*-BMA) copolymers. For the clean polymers, the two separate T_g values were observed. This result can be explained as follows. The presence of DOP plasticizer

TABLE VII
Recipe and Experimental Results of Styrene and Butyl Acrylate Copolymerization Using an SPG Pore Size of 0.90 μm

Run no.	Composition	Monomer composition (wt %)	Monomer conversion (%)	D_e (μm)	CV_e (%)	D_p (μm)	CV_p (%)	$\overline{M}_n$ ($\times 10^{-4}$)	$\overline{M}_w$ ($\times 10^{-4}$)	PDI	T_g (°C) Clean	T_g (°C) Unclean
2048	P(St-*co*-BA)	75/25	71.3	8.7	13.9	6.2	15.8	2.6	6.2	2.4	22.7/58[a]	17.4/51.6[a]
2047	P(St-*co*-BA)/ DOP	75/25	65.1	8.1	15.1	6.5	16.3	2.1	4.9	2.3	40.2	16.8
2049	P(St-*co*-BA)/ PSt	(62.5/25)/12.5	86.0	7.6	13.5	5.3	17.4	0.7	3.9	5.4	17.2/55[a]	18.8/52.0[a]
2050	[P(St-*co*-BA)/PSt]/ DOP	(62.5/25)/12.5	67.9	6.8	21.7	5.2	23.3	0.6	3.7	5.9	22.2/53.3[a]	19.7

[a] Two separate T_g values were observed.

in the copolymer depends largely on the physical interaction between the copolymer and the plasticizer. After the solvent washing, DOP could remain partially in the polymer particles, if this interaction is strong enough.

Effect of DOP on properties of poly(St-*co*-BA) copolymer

The SPG membrane with a pore size of 0.90 μm was used for emulsification of the St and BA monomers. The experimental results are shown in Table VII and Figure 8. The presence of the soft BA phase in the copolymer synergistically enhances the plasticizing effect of DOP. Because BA itself behaves like a plasticizing monomer, the expected single glass-transition temperature was found in poly(St-*co*-BA) particles for both clean and unclean samples (Run 2047). However, when PSt was added into the St–BA monomer mixture, the synthesized poly(St-*co*-BA)/PSt gave a single T_g value in the unclean particles. For the clean particles, two separate T_g values were found. Likewise, a low number-averaged molecular weight was also found, as in the above-mentioned case of poly(St-*co*-BMA).

Internal morphology of poly(St-*co*-MA)

The microtomes and stained polymer particles (Runs 2018 and 2019) reveal their internal morphology as shown in Figure 9. The internal particle morphology was observed by varying the monomer composition. The transmission electron micrographs of poly(St-*co*-MA) with St/MA of 75/25 and 50/50 are shown in Figure 9(a), (b). Inside the particles, the small white granules of MA were revealed. The granules did not appear at the outermost submicron thickness at the circumference of the particle. When a higher concentration of styrene was incorporated, larger sizes of white granules were produced as shown in Figure 9(b).

When the emulsion droplets are formed, there is a time lapse before the subsequent suspension polymer-

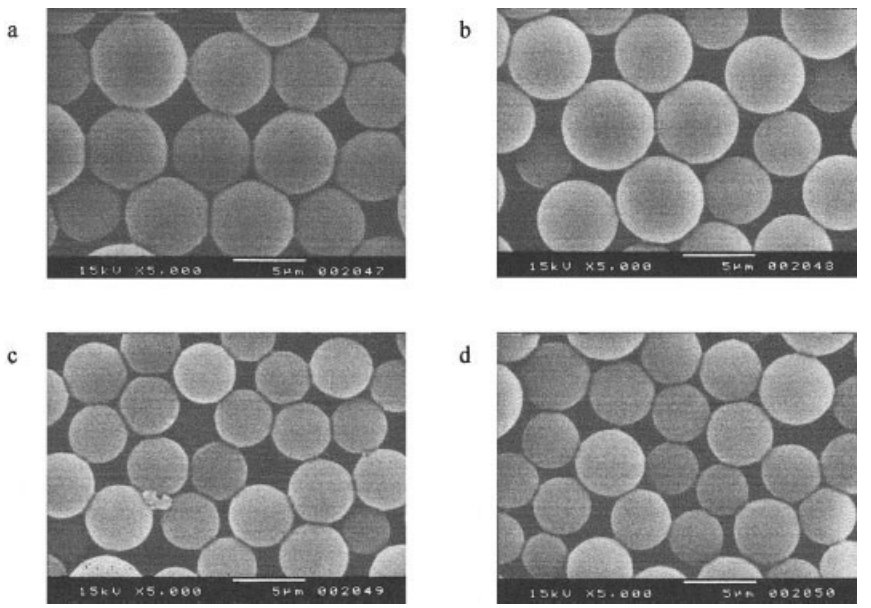

Figure 8 SEM micrographs of polymer particles: (a) poly(St-*co*-BA), St : BA = 75 : 25; (b) poly(St-*co*-BA)–DOP, St : BA = 75 : 25; (c) poly(St-*co*-BA)/PSt, St : BA : PSt = 62.5 : 25 : 12.5; (d) poly(St-*co*-BA)/PSt, St : BA : PSt = 62.5 : 25 : 12.5.

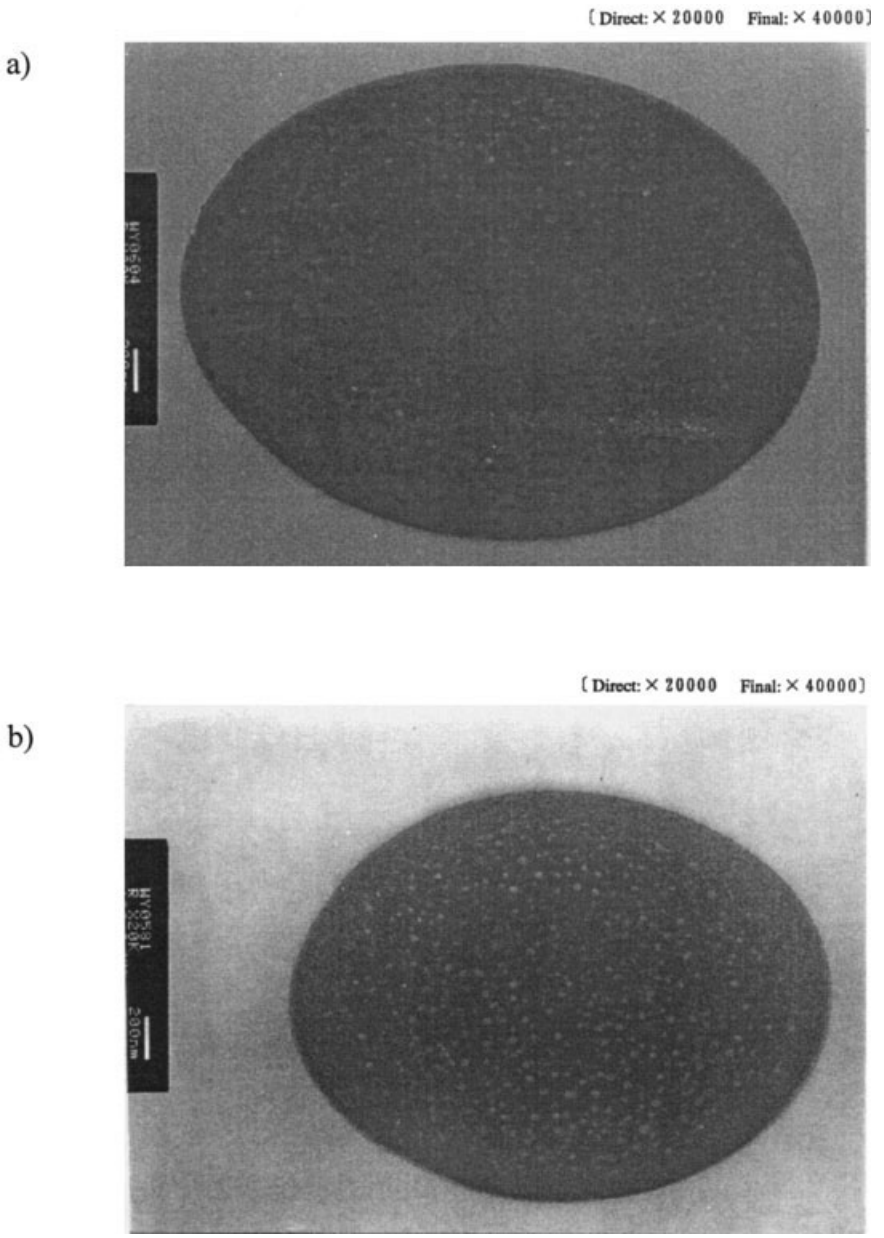

Figure 9 TEM micrographs of poly(St-*co*-MA): (a) St : MA = 50 : 50; (b) St : MA = 75 : 25.

ization. We observed some droplet separation and their suspension inside the larger drops. Given that the MA reactivity ratio is greater than that of styrene, MA monomer droplets were consumed faster at the beginning of the polymerization to become the small domains. The styrene-rich phase was subsequently produced, which later became the matrix for the MA domains. The TEM micrographs also suggest that some diffusion of MA-rich domains into the styrene-rich polymer matrix probably occurs.

CONCLUSIONS

SPG emulsification and subsequent suspension polymerization were employed for preparation of two-phase styrene–acrylate copolymer particles incorporating DOP plasticizer. Both suspension and emulsion polymerizations took place, but the former controls the polymer behavior. The presence of DOP on the polystyrene-based particles significantly enhances the mobility of the styrene backbone and yields lower T_g values of the copolymers. The slightly nonpolar DOP preferentially plasticizes the matrix phase of both the hard PS-phase and the soft (meth)acrylate-phase. Regardless of the monomer concentration ratios, the resulting spherical polymer particles range in size from 3 to 7 μm. Upon washing the polymer particles with methanol, DOP in the polymers was washed out and two separate T_g peaks resulted. Microphase separation was found when the monomer droplets were formed

at a later stage in the emulsification process. Small particles were then produced to give a broad molecular weight distribution.

All the comonomer pairs under study exhibited composition drift during the copolymerization because of their substantial difference in monomer reactivity ratios, which was evidenced by the T_g values of the copolymers. In comparison, poly(MMA-*co*-MA) revealed that they were well compatabilized with DOP. A single T_g value with a sharp transition was found in both clean and unclean particles, given that the presence of a similar functional group (ester) significantly enhances the physical interaction between them and yields more compatible behavior. When the low T_g polymers are carefully produced, the polymer particles can be used for surface-coating purposes without the inclusion of plasticizers because film flexibility and a low glass-transition temperature can be obtained directly from the inherent properties of the designed monomers and their corresponding copolymer. In addition, the inclusion of moderately high molecular weight polystyrene in the polymerization solution and the effect of DOP as a plasticizer for the copolymer, based on the polymer particle properties and glass-transition temperature, are not significant.

The authors express their sincere appreciation to the Golden Jubilee Program of the Thailand Research Fund for providing a scholarship through Contract Number 2.M.CU/42/E.1, and to the Graduate School of Bio-Applications and Systems Engineering (BASE), Tokyo University of Agriculture and Technology, Tokyo, Japan for providing research facilities to the first author to carry out this research.

References

1. Landfester, K.; Spiess, H. W. Acta Polym 1998, 49, 451.
2. Winnik, M. A.; Feng, J. J Coat Technol 1996, 68, 39.
3. Cho, I.; Lee, K. W. J Appl Polym Sci 1985, 30, 1903.
4. Min, T. I.; Klein, A.; El-Aasser, M. S.; Vanderhoff, J. W. J Polym Sci Polym Chem Ed 1983, 21, 2845.
5. Nelliappan, P.; El-Aasser, M. S.; Klein, A.; Daniels, E. S.; Robert, J. E. J Polym Sci Part A: Polym Chem 1996, 34, 3173.
6. Chen, Y. C.; Dimonie, V. L.; El-Aasser, M. S. J Appl Polym Sci 1991, 42, 1049.
7. Jonsson, J. E.; Hassander, H.; Tornell, B. Macromolecules 1994, 27, 1932.
8. Jonsson, J. E.; Karlsson, O. J.; Hassander, H.; Tornell, B. Macromolecules 2001, 34, 1512.
9. Stubbs, J.; Larsson, O.; Jonsson, J. E.; Sundberg, E.; Durant, Y.; Sundberg, D. Colloids Surf A: Physiochem Eng Aspects 1999, 153, 255.
10. Shieh, Y.; Liu, C. M. J Appl Polym Sci 2002, 83, 2548.
11. Hsu, S. C.; Lee, C. F.; Chiu, Y. C. J Appl Polym Sci 1999, 71, 47.
12. Feng, J.; Winnik, M. A.; Shivers, R. R.; Clubb, B. Macromolecules 1995, 28, 7671.
13. Tamai, T.; Pinenq, P.; Winnik, M. A. Macromolecules 1999, 32, 6102.
14. Kirsch, S.; Pfau, A.; Stubbs, J.; Sundberg, D. Colloids Surf A: Physiochem Eng Aspects 2001, 183, 725.
15. Nuisin, R.; Ma, G. H.; Omi, S.; Kiatkamjornwong, S. J Appl Polym Sci 2000, 77, 1013.
16. Sudol, E. D.; El-Aasser, M. S.; Vanderhoff, J. W. J Polym Sci Part A: Polym Chem 1986, 24, 3515.
17. Brandrup, J.; Immergut, E. H. Polymer Handbook, 3rd ed.; Wiley: New York, 1989; Sec. II, pp. 182–216.
18. Odian, G. Principles of Polymerization, 3rd ed.; Wiley: Singapore, 1991; pp. 460–466.
19. Zhao, Y.; Urban, M. W. Macromolecules 2000, 33, 8426.
20. Kiatkamjornwong, S.; Nuisin, R.; Ma, G. H.; Omi, S. Chin J Polym Sci 2000, 18, 309.